

## Optimal Design and Performance Analysis of a Grid Connected Microgrid System

<sup>1</sup>P. D. Singh, <sup>2</sup>Ajay Upadhaya, <sup>3</sup>Michael Simte and <sup>4</sup>Abhishek Sanyal

Department of Electrical Engineering, North Eastern Regional Institute of Science and Technology, Nirjuli, INDIA

E-mail: <sup>1</sup>[pds@nerist.ac.in](mailto:pds@nerist.ac.in), <sup>2</sup>[ajayupadhaya17@gmail.com](mailto:ajayupadhaya17@gmail.com), <sup>3</sup>[michaelbsimte@gmail.com](mailto:michaelbsimte@gmail.com), <sup>4</sup>[avisanyal6666@gmail.com](mailto:avisanyal6666@gmail.com)

### ABSTRACT

Microgrid (MG) is the vital component in the future global smart power system. The study of any MG system is utmost important as it presents ideas of integrating green energy in the electrical power system. This work aims to integrate some amount of renewable energy from solar photo voltaic system with an energy storage device to supplement the load demand of a selected local area. The expected generation from such sources is estimated and also determined the amount of energy which could be shared to the local local demand. The study considers a MG system operated in grid-connected mode which means the total load is being shared by the sources in the system as well as main grid. Hence, the first part of the study focuses on the design of an optimum MG system based on a given load data and available resources for minimum cost of energy, maintenance and replacement by using HOMER Simulation software. The system is so designed has the most efficient distributed sources and optimum ratings of the components required to meet the required load demand. Secondly, the system is modelled and simulated in MATLAB/Simulink to study the performances of the operation of the MG system so designed including power quality analysis.

**Keywords:** *Distributed Energy Resources, Grid Connected Microgrid System, Maximum Power Point Tracking (MPPT), Solar Photo Voltaic, Energy Storage System, Boost Converter*

### 1. INTRODUCTION

With the ever-increasing demand of electricity and degrading environment on the other hand, it becomes necessary to integrate more and more renewable energy resources in the conventional power system. Renewable energy resources are available in the form distributed energy known as Distributed Energy Resources (DERs) which include Photo Voltaic System, Wind Energy System, Small Hydro Power Generations, Fuel cells, Biomass, etc [6, 7]. Hence, Microgrid (MG) can be formed by a few numbers of such DERs and such a system can meet the load demand of any feasible location. Depending on the accessibility of the location with the main grid, the MG so may be designed can either feed the local load only to operate in Islanded Mode or may also inject excess power to the main grid to operate in Grid Connected Mode [7, 8, 9]. In this work, the operation of the MG system in Grid Connected Mode is considered while feeding a share of the total load demand of a defined location by MG system consisting of PV system and Battery Storage System. The DERs need to be regulated properly with the help of power electronics controllers to maintain constant voltage during variations in load and generation [10]. A solar PV system operates at low DC voltage which needs to be stepped up with the help of a boost converter before supplying to the DC bus [1, 3]. A maximum power point tracking (MPPT) controller is employed to provide maximum power from the PV module. In one of the studies, two such algorithms are presented for MPPT known as Perturb-and-Observe Method and Incremental-Conductance Method respectively [4, 11]. A bidirectional converter is required between the DC bus and the AC bus. Parallel-connected bi-directional converters for DC and AC hybrid MG application are proposed for efficient interfacing [2]. A storage unit consisting of battery is included to maintain

stability during transient and load variations. A charge controller is used for controlling the battery to charge and discharge during excess and shortage of power respectively [5].

The objectives of the whole work are divided into two parts; firstly, it presents an optimum design of MG system after gathering all the resources using HOMER simulation software. The MG system consists of PV array system, a MPPT with boost converter for PV array, a battery with bidirectional charge controller, a three-phase inverter to convert DC to AC power, transformer and local load connected to the main grid. Secondly, the optimum MG system so designed in Homer is now modelled and simulated in MATLAB Simulink for performance analysis including power quality analysis.

### 2. SIMULATION MG SYSTEM USING HOMER SOFTWARE

In the first part of the paper, the design of the MG system is carried out by using Homer Pro. Homer Pro offers advantages as it can obtain some technical data already available based on the location such as Wind Speed data, Sunshine records, Rainfall data, Temperature, etc. [7]. Besides, there are options to employ either real time components or user defined ones. The various prerequisite resources of data required for the design such as temperature records on daily, monthly and yearly basis, Wind profiles, Solar Radiation records, etc. are collected from the server of NASA. Based on the profiles of various resources obtained for a selected local area, appropriate components sizing is done. Finally, the simulation is carried out as per the load

demand profile for the local area under consideration to obtain the optimum MG system design.

**A. Electric Load Profile**

The energy consumed by the locality under study is found to be 537 kWh/day with peak demand of 55.24 kW and load factor of 0.41 with random variability day to day of 5%. The load profiles for the specified system can be shown by HOMER in Figure 1. The load is at its peak from 7 pm to 8 pm and minimum between 12 am to 3 am.

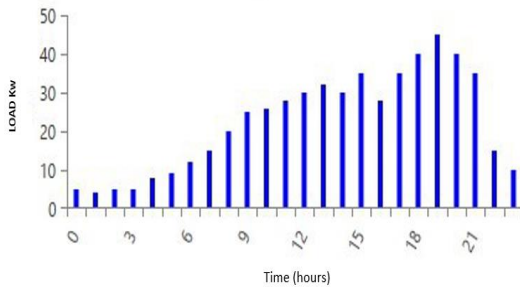


**Figure 1.** Daily Load Profile of the Area

**B. Design Considerations**

Based on the load assessments, the MG design considers a system including a Generic PV, 1kWh Li-Ion Storage Batteries, Converter, Load and Grid as shown in Figure 2. The complete system descriptions viz. Solar resource, Temperature resource and detail of the various components are discussed in the following sub-headings.

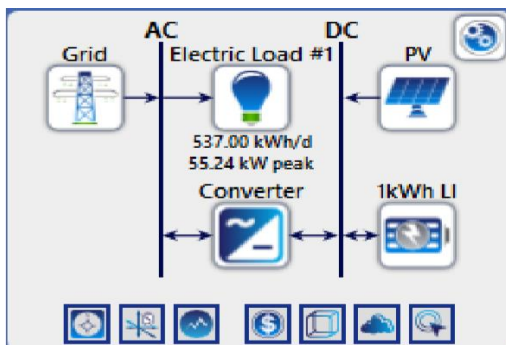


**Figure 2.** Schematic Diagram Showing Various Components of Microgrid System

**C. System Specifications**

The monthly average radiation data for a period of one year is obtained by specifying the coordinates of the area under consideration i.e. 27.1°N 93.62°E. It has a relatively strong solar resource with a daily radiation annual average of 3.95 Kwh/m<sup>2</sup>/day with the highest values of solar radiation ranging from April to June. Similarly, the monthly average temperature profile is obtained and an annual average temperature is found to be 23.89 °C. The temperature ranges are higher during April to August. Series-parallel connected PV module of 1 kW Generic flat type is considered. The yearly maintenance cost and the de-rating factor are considered as \$5 and 90% respectively. The sizing for simulation is provided by Homer Optimizer. Another component of the system is the energy storage device for which a battery bank with a capacity sufficient enough to store energy for operating the load during cloudy days and night times is designed. A lead acid battery bank of 24 V, 167 Ah/kWh with round trip efficiency of 90% is considered for the purpose. A bidirectional generic system converter of 1 kW with efficiency of 95% is considered. Load Following dispatch (LF) controller is implemented with its algorithm design to utilize optimum energy supply from the main grid except during shortage of power from DG sources. When power generated is less than load demand, power may be taken from grid or else it injects excess power to the grid. The sale capacity to the grid is defined along with suitable grid interconnection and extension charges.

**3. MG DESIGN BY HOMER SIMULATION SOFTWARE**

Based on assessments of all the resources data and after defining all the feasible ranges of ratings of PV System, Battery System and Converter System connected to the local load and grid, simulation is carried out in Homer Optimizer. 861 numbers of results are found out in which 612 numbers are found to be feasible. The results are arranged according to the minimum total net present cost (NPC) as shown in Figure 3. The configuration consisting of PV system and Grid is found in the first row of the results. However, the second configuration is considered viable due to advantages of having an energy storage system though it has a slightly higher NPC compared to the first configuration. It is also

Architecture					Cost				S <sub>1</sub>			
PV (kW)	1kWh LI	Converter (kW)	Dispatch		NPC (\$)	COE (\$)	Operating cost (\$/yr)	Initial capital (\$)	Ren Frac (%)	Total Fuel (L/yr)	Capital Cost (\$)	Production (kWh/yr)
101		61.4	LF		\$212,094	\$0.0681	\$10,520	\$76,102	51.3	0	60,525	143,039
103	24	61.8	LF		\$218,875	\$0.0700	\$10,380	\$84,684	52.0	0	61,822	146,104
			LF		\$253,968	\$0.100	\$19,622	\$300.00	0	0		
	24	0.0648	LF		\$270,933	\$0.107	\$20,145	\$10,513	0.00883	0		

**Figure 3.** Simulation Result

advantageous compared to all other cases as it has lowest operating cost and increased energy production despite slightly higher Cost of Energy (COE) and capital cost. Moreover, the CO<sub>2</sub> emission Capital Expenditure (CAPEX) and Operational Expenditure (OPEX) are also found lesser than any other configurations except first configuration. The project is designed for 25 years and the lifetime of all the components are assumed to be 25 years. Since the electricity

produced, stored and supplied from the grid are shared, there is no unit of energy demand left unmet. PV system has an annual production of 143224 kWh out of total 259729 kWh annual production and the remaining is contributed from the main grid. The simulation results give a rated capacity of PV modules as 103 kW for supplying the load demand at a capacity factor of 16.2%.

The optimum size of the battery system is obtained for 24 numbers of 24 V batteries with 4 series batteries in a string and 6 parallel strings. The battery system has an energy inflow rate of 7239 kWh/yr and outflow rate of 6533 kWh/yr. The converter losses if found to be 6533 kWh/yr. The grid energy exchange detail is shown in Table 1.

performance analysis as shown in Figure 4. Each components including PV system, MPPT, VSI, boost converter, buck-boost converter, battery, LC filters, load of the MG system are modelled based on the parameters obtained from the HOMER optimization [12]. Further, a grid connected MG system is considered where the load can be supplied either by the PV system/battery system or the grid. For the purpose of study, a linear load of 55.24 kW is connected and disconnected at certain times to observe the performances. Secondly, the performance analysis is also done for the case of resistive and inductive (RL-load). For RL- load, an R-load of 30 kW and L-load of 10 kVAR is considered for the study which is connected to the system at 2.5 Sec and disconnected at 5 Sec. The detail performance analysis of the simulation results are discussed in Section 5.

**Table 1** Grid Exchange Rate

Time Period	Energy IN (kWh)	Energy OUT (kWh)	Net Energy IN (kWh)	Peak Demand (kW)	Energy Bill (\$)	Demand Bill (\$)
Yearly	116,505	44,631	71,874	55.2	9,419	31.25

#### 4. MATLAB SIMULATION FOR PERFORMANCE ANALYSIS OF MG SYSTEM

The Matlab Simulink model of the optimized MG system obtained in HOMER Software is now developed for

##### A. PV system

Solar PV is used as the main power source in this microgrid which is further used to maintain the DC Link voltage of 500V using boost converter. PV array used consists of 66 modules in parallel with 5 strings in series. The power rating of each module is 305 W. The rated power of PV system is about 100 kW. The V-I and P-V characteristics

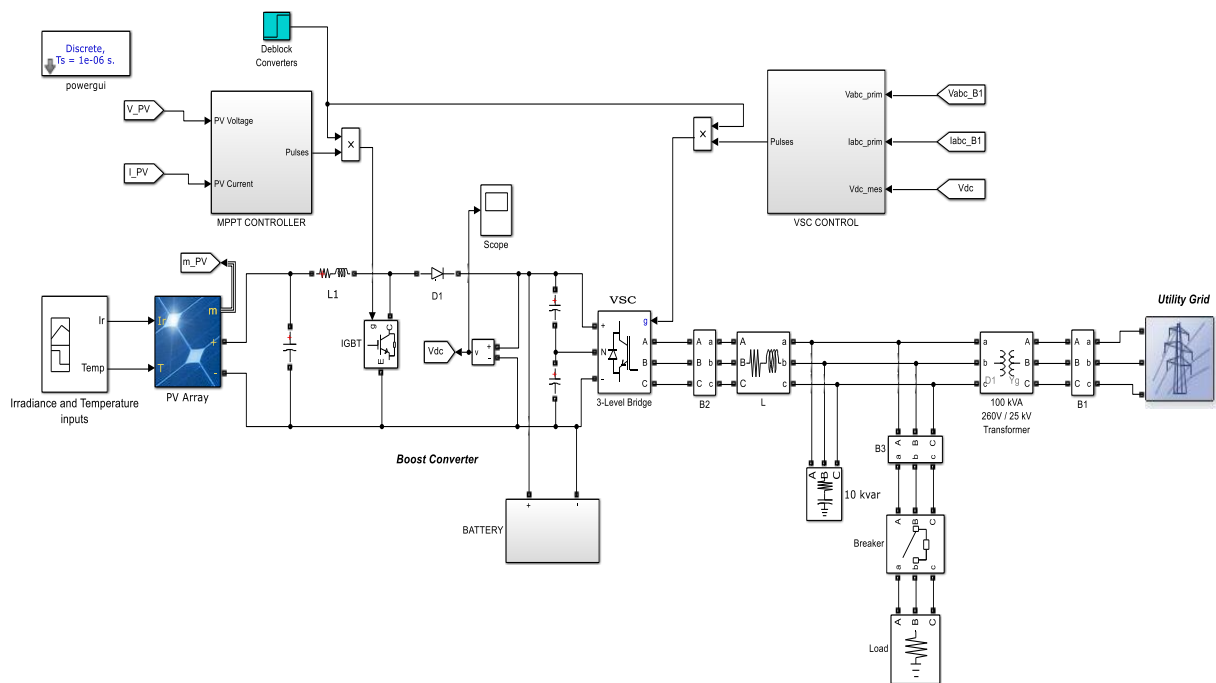


**Figure 4.** Simulink Diagram of the proposed MG System

of the PV module used in the system are given in the Figures 5 and 6.

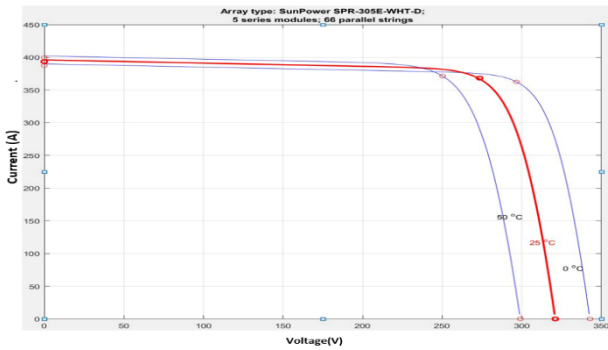


**Figure 5.** I-V curve showing Maximum Power Point Tracking

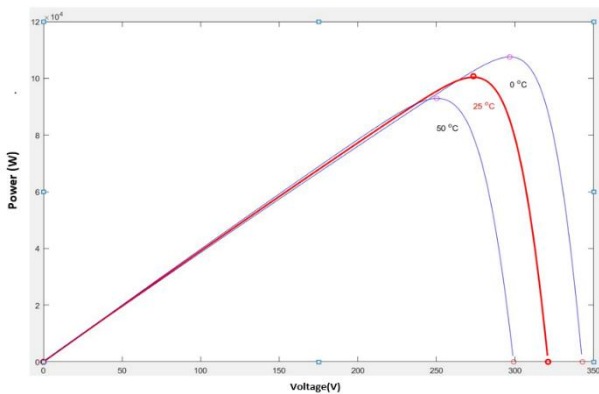


**Figure 6.** Power and Voltage Curve showing the “Knee” value

**B. Boost Converter**

The DC-DC converter as shown in Figure 7 is connected at the output of the PV array to operate in boost

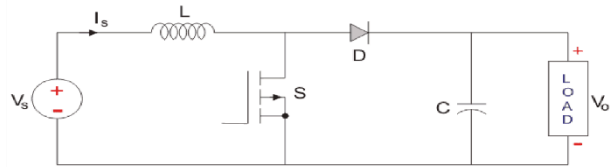


**Figure 7.** Boost converter circuit

mode. This DC-DC boost converter in conjunction with MPPT controller ensures maximum power and constant DC Link voltage [11]. The MPPT uses Incremental and Conductance algorithm. The capacitor is connected in parallel to reduce the voltage ripple.

$$V_o = V_{in} / D \dots\dots\dots (1)$$

Where  $V_o$  is the output voltage and  $V_{in}$  is the input voltage and  $D$  is the duty cycle. Hence, by controlling the duty cycle can be controlled the output voltage required for DC Link voltage. The duty cycle for the IGBT switch is controlled using MPPT control.

**C. MPPT**

Maximum power point tracking (MPPT) is used to extract maximum power from the PV at varying irradiance and temperature. The working of the MPPT algorithm is depicted in the flowchart given in Figure 8.

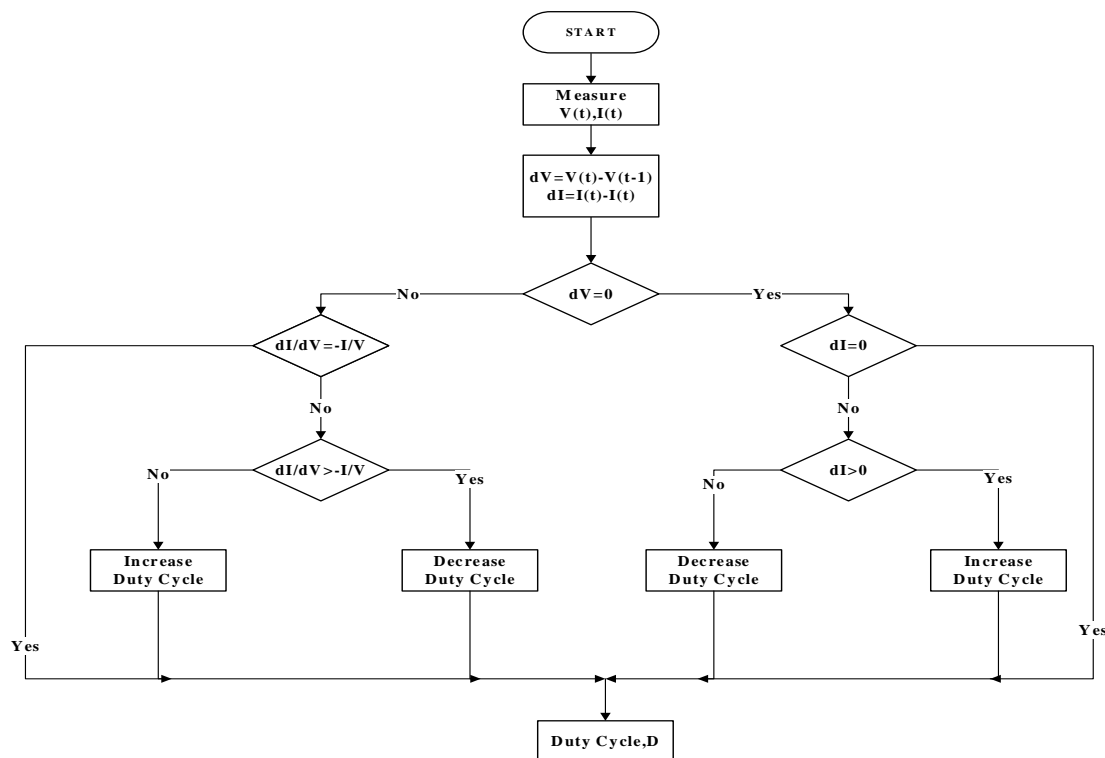


**Figure 8.** MPPT Flowchart

The Incremental Conductance algorithm is used to find the point that gives the equation for maximum power possible from the PV module. The algorithm uses the following equation

$$P = V \times I \dots\dots\dots(2)$$

where P is output power, V is PV voltage and I is PV current. Differentiating with respect to dV

$$\frac{dP}{dV} = \frac{dI}{dV} + I \dots\dots\dots(3)$$

At maximum power point

$$\frac{dP}{dV} = 0 \& \frac{dI}{dV} = -\frac{I}{V} \dots\dots\dots(4)$$

For the operating point in the right side of the power curve, we have

$$\frac{dP}{dV} < 0 \& \frac{dI}{dV} < -\frac{I}{V} \dots\dots\dots(5)$$

When the MPPT has achieved the maximum power point, the algorithm directs to stop perturbing the operating point. Otherwise, if it is not achieved, then MPPT algorithm follows the direction as computed by dI/dV and -I/V relation. The algorithm is implemented in the Matlab using the blocks as shown in Figure 9.

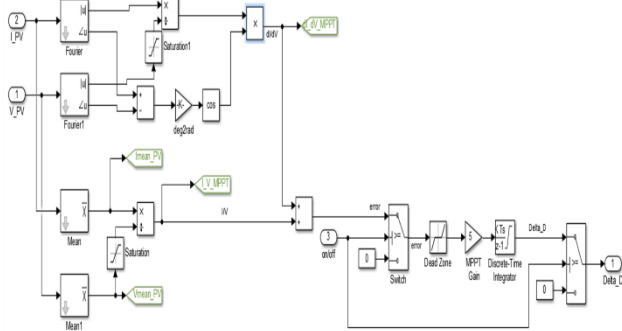


Figure 9. Algorithm of MPPT in Matlab/Simulink

Table 2 shows the maximum powers that can be extracted at different temperature and irradiance.

Table 2 Maximum power extractable at different temperature and irradiance

Irradiance (W/m <sup>2</sup> )	Temperature (°C)	PV Voltage (V)	Maximum Power Output (kW)
1000	25	273.5	100.7
1000	50	250.2	92.9
250	25	265.1	24.4

D. Battery System

The battery uses DC-DC bi-directional converter and the controller which helps the battery in charging and discharging depending on the power variations. The DC-DC Bidirectional Converter is used to step down or step up the voltage for battery charging and discharging respectively. During excess generation the converter operates to charge

the battery in buck mode and during shortage of generation it operates in boost mode for to discharge it.

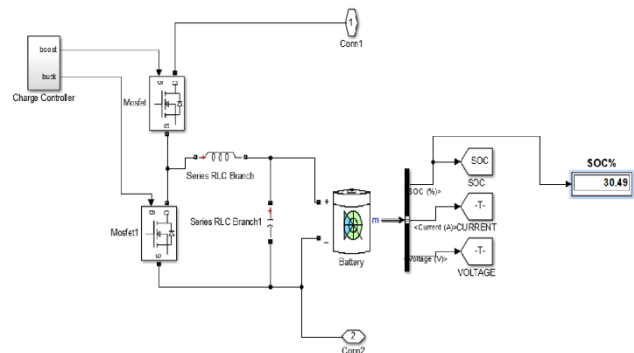


Figure 10. Simulation Battery System in Matlab Simulink

E. AC/DC Bidirectional Converter

AC/DC bidirectional converter enables bidirectional power flow between the DC link and AC side of the grid. This along with its control allows us to stabilize DC link voltage to a constant value. This converter uses IGBT as switching devices and uses switching frequency of 10 kHz.

F. Voltage Source Converter (VSC) Control

The grid side control algorithm is developed to maintain the dc link voltage and the power factor by de-coupling d and q components of the current and synchronizing the frequency using Phase Locked Loop (PLL). The d and q components are obtained from the three phase values using Park's Transformation. The comparison of measured and reference values of d and q components is fed to the current regulator and subsequently generates a reference voltage set as shown in Figure 11. Thus, the PWM generator gets the required signals to trigger the IGBT switches of the VSC.

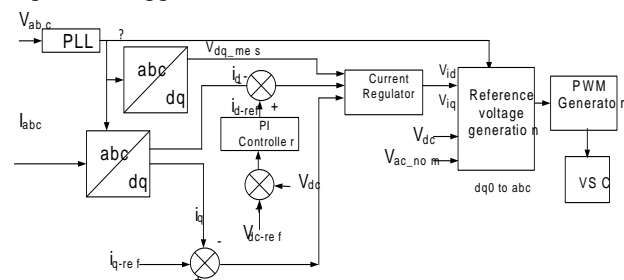
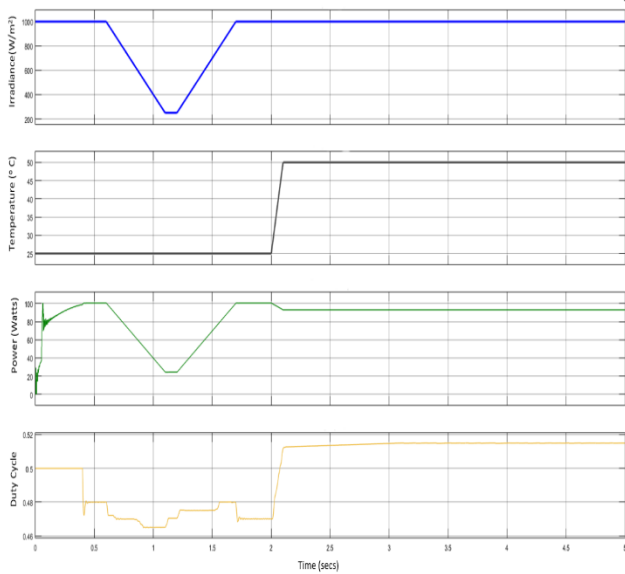


Figure 11. Implementation of VSC Control

5. MATLAB SIMULATION RESULTS AND PERFORMANCE ANALYSIS OF MG SYSTEM

A hybrid microgrid whose optimized parameters obtained using HOMER software is modelled in MATLAB/Simulink platform. Then performance of the MG system including photovoltaic system and battery with grid connection is analysed. The solar irradiation and cell temperature variations are considered for the study as shown

In Figure 12. The MPPT in the photovoltaic (PV) system allows the PV modules to extract the optimum power. It uses the Incremental and Conductance algorithm to track the point for producing maximum power by the PV module. Figure 12 shows that when the temperature



**Figure 12.** Tracking of Maximum Power Point and the duty cycle during variation of temperature and Irradiance

and irradiance are changed the MPPT tracks the maximum point and tries to change the duty cycle. The change in the duty cycle in search of maximum power can be seen in the figure given above. PV system does not provide constant output due to varying temperatures and irradiances at different times and hence, the unregulated dc output voltage varies in the range of 273.5 V to 250.2 V. Therefore, a boost converter is used to maintain dc link voltage constant at about 500 V to give the desired output level. The battery uses the DC-DC bidirectional converter and the controller which helps the battery in charging and discharging depending on the SOC of the battery. The DC-DC Bidirectional Converter is used to bring down the voltage from 500 V to 24 V for Battery charging in Buck mode and step up the voltage from 24 V to 500 V while discharging in boost mode. The State of Charge (SOC) conditions during charging and discharging processes are tested and found working as shown in Figures 13 and 14.

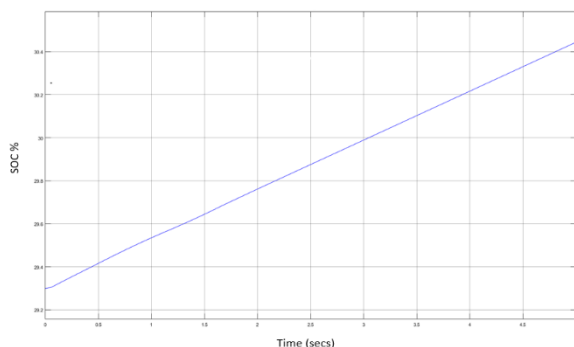


**Figure 13.** Charging process represented by increase in SOC w.r.t time

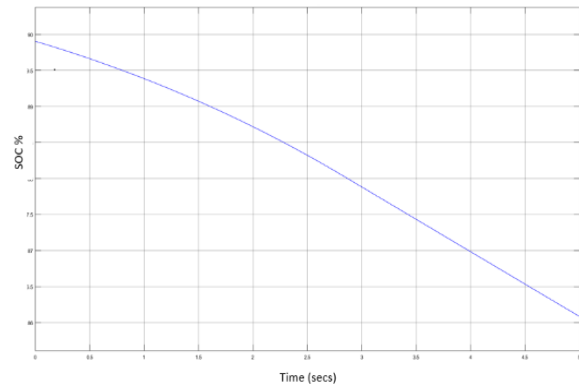


**Figure 14.** Discharging process represented by decrease in SOC w.r.t time

The performance analysis is done using simulation results under two cases of loadings. Firstly, a resistive load (R-load) of 55.24 kW is connected at 2.5 sec and disconnected at 5 sec. In the second case, an inductive load of (RL-load) of 30 kW and 10 kVAR is connected at 2.5 sec and disconnected at 5 sec. The results and discussions are presently as follows. From Figure 15, it can be seen that the peak voltage is around 367 V and the RMS voltage is 254.1 V and the rms current is about 1.2 A during loading of R-load. At no load condition, the peak and rms voltage are 381.7 V and 257.5 V respectively.

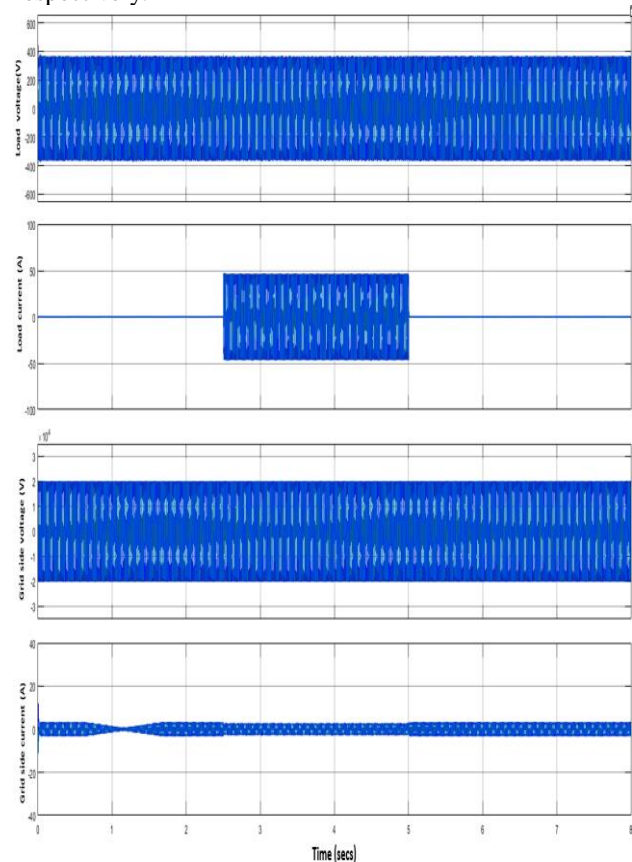


**Figure 15.** Waveforms of Output Voltages and Currents under R-load condition

At RL-load, the load side rms voltage and current are found to be 256.7 V and 18.43A respectively and that of the grid side are 13.93 kV and 1.928 A respectively as shown in

Figure 17. The DC link voltages for both the cases are found to be maintained nearly at 500 V as shown in Figures 16 and 18.

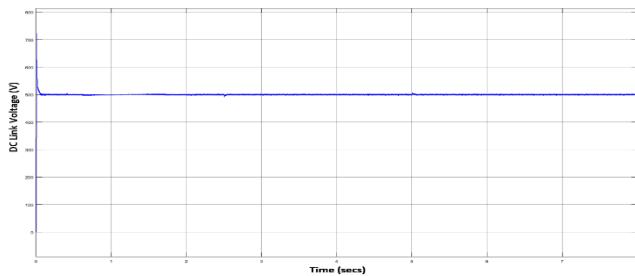


Figure 16. DC link Voltage during R-load

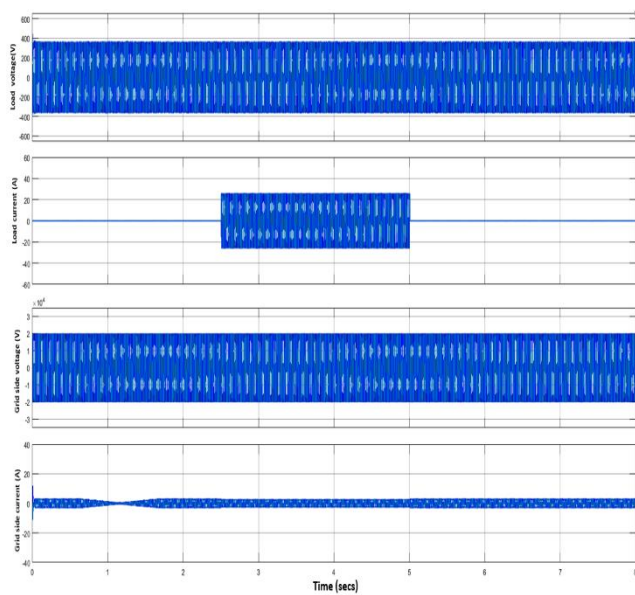


Figure 17. Waveforms of Output Voltage and Current under RL-load condition

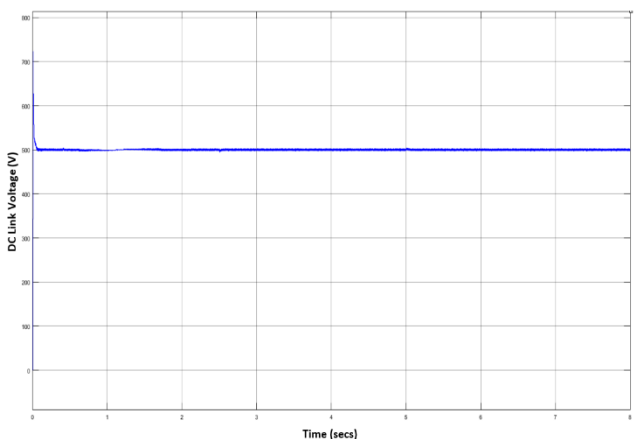
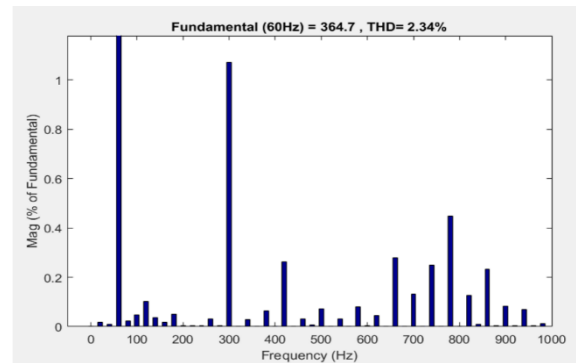
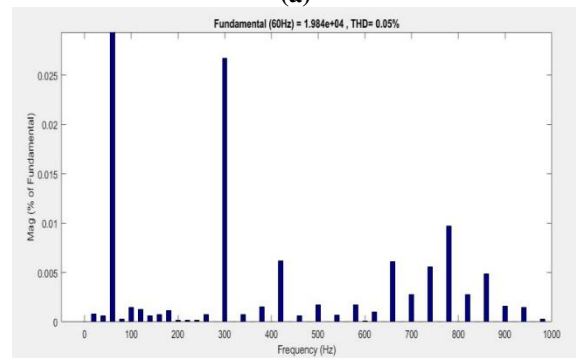


Figure 18. DC link Voltage under RL-load condition

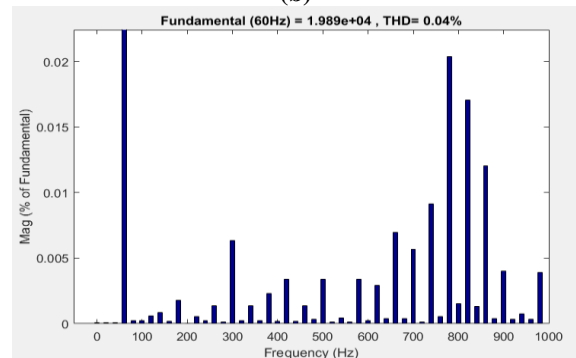
The Inverter output voltage contains THD of 33.11%. An LC filter is used to arrest this high level of harmonics. LC filter reduces the THD values to 2.34% on load side and 0.05% at grid side for the case of R-load and 0.04% and 2.22% at load and grid sides respectively for the case of RL-load. The FFT analysis reveals the reduction in the THD values as shown in the Figure 19.



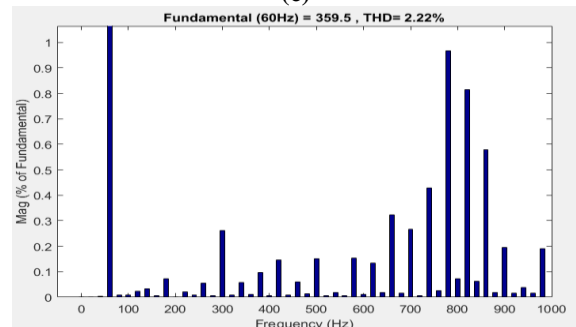
(a)



(b)



(c)

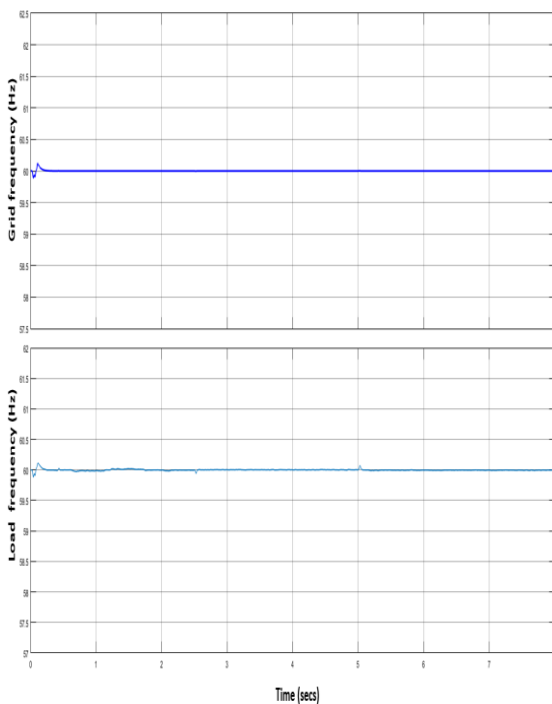


(d)

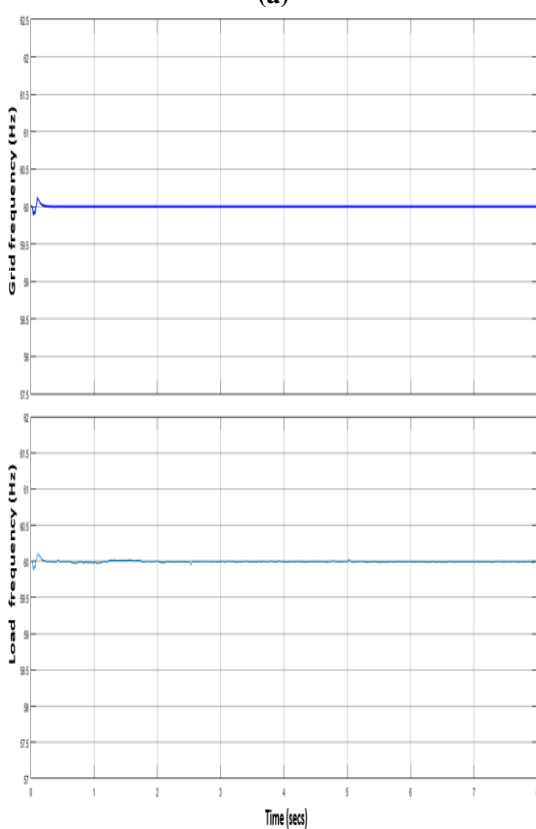
Figure 19. FFT analysis of voltage waveform at (a) Grid side for R-load (b) Load side for R-load (c) Grid side for RL-load (d) Load side for RL-load

In all the cases, the system frequency is found to be stable at rated frequency i.e. 60 Hz as shown in Figure 20. Initially, the frequency of the system is fluctuating from  $t=0$  sec to  $t=0.05$  sec as there is no pulse given to the switches of the inverter. As soon as the pulses are developed after  $t=0.05$  sec, the frequency slowly comes to steady at the value

of 60 Hz as the desired frequency which means that PLL synchronizes the frequency at 60 Hz.



(a)

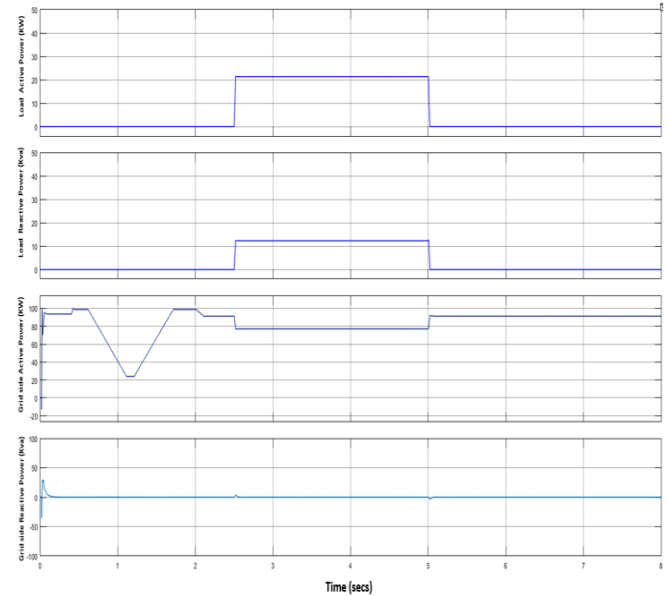


(b)

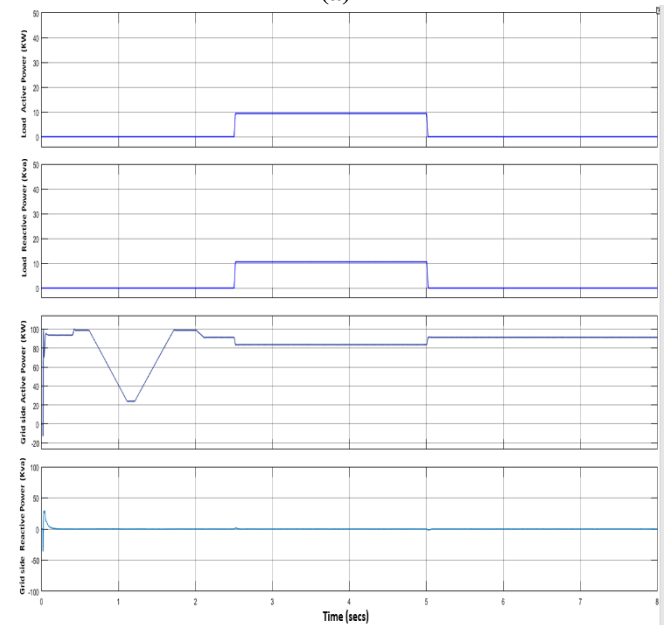
**Figure 20.** (a) System Frequency for the case of R-load  
(b) System Frequency for the case of RL-load

The active and reactive power flow at load and grid sides for the two cases of loadings are found to be steady and optimum  
ITEE, 8 (3) pp. 74-82, JUN 2019

as depicted from Figure 21 (a) and (b). There are slight fluctuations during the starting of the simulation as all the controllers are tuning to set at the steady state conditions which are also visible in the case of waveforms of powers.



(a)



(b)

**Figure 21.** (a) Active and Reactive Power Flow for the case of R-load (b) Active and Reactive Power Flow for the case of RL-load

## 6. CONCLUSION

After comparison among various configurations provided in the simulation result of HOMER PRO, the optimum design of MG system is determined. It is found that the system design consisting of 103 kW Solar PV, 24 kWh capacity battery storage system and 61.8 kW rated converter MG system connected to grid gives optimum results. It has minimum Net Present Cost (NPC) and Cost of Energy (COE) compared to that of the other cases. Also, it offers least CO<sub>2</sub>



emission of 73.631 kg/yr. The However, the MG system so designed has only about 55% energy contribution to the total energy required and the remaining is fed from the main grid. The integration of more DGs may help improving the percentage shared by renewable energy. In the next part of the study, the optimum design of MG system obtained in the Homer Software is modelled in the Matlab Simulink. The model consists of PV array, boost converter, DC-DC and DC-AC bidirectional converters, MPPT algorithm, LC filters and the grid system. The various waveforms such as voltage, current, active and reactive power waveforms are obtained and found to be stable and optimum. The output voltages and frequency are maintained at rated values during various loading conditions. For all the cases, the FFT analysis of the output voltages at grid and load sides show that the %THD values are well within the prescribed limits of IEEE standards [13]. Thus, in all, this paper has presented an approach to design an efficient Microgrid system to meet the load demand of a proposed residential load and its performance analysis has shown that the system is feasible and efficient. Future studies may incorporate some more renewable energy resources like small hydro power plants, wind energy, biomass, fuel cells, etc. to further reduce the load shared by the main grid.

## REFERENCES

- [1] A. Muhtadi and A. M. Saleque, "Modeling and simulation of a microgrid consisting solar PV & DFIGN based wind energy conversion system for St. Martin's island," 2017 IEEE 3rd International Conference on Engineering Technologies and Social Sciences (ICETSS), Bangkok, 2017, pp.1-6.
- [2] E. C. dos Santos, "A bidirectional dc-ac converter," IECON 2012 - 38th Annual Conference on IEEE Industrial Electronics Society, Montreal, QC, 2012, pp. 50-56.
- [3] R. AbdelHady, "Modeling and simulation of a micro grid-connected solar PV system," Water Sci., vol. 31, no. 1, pp. 1-10, 2017.
- [4] G. Alvarez, H. Moradi, M. Smith and A. Zilouchian, "Modeling a Grid-Connected PV/Battery Microgrid System with MPPT Controller," 2017 IEEE 44th Photovoltaic Specialist Conference (PVSC), Washington, DC, 2017, pp. 2941-2946".
- [5] S. Adhikari and F. Li, "Coordinated V-f and P-Q Control of Solar Photovoltaic Generators With MPPT and Battery Storage in Microgrids," in IEEE Transactions on Smart Grid, vol. 5, no. 3, pp. 1270-1281, May 2014.
- [6] Fei Ding, Peng Li, Bibin Huang, Fei Gao, Chengdi Ding and Chengshan Wang, "Modeling and simulation of grid-connected hybrid photovoltaic/battery distributed generation system," CICED 2010 Proceedings, Nanjing, 2010, pp. 1-10.
- [7] P. Gilman and P. Lilienthal, "Micropower system modeling," in John Wiley & Sons, Inc, 2006, pp. 379-418.
- [8] R.H.Lasseter, "Micro-grids", IEEE Power Engineering Society Winter Meeting, Vol.01, pp. 305- 308, New York, NY, 2015
- [9] A. Banerji et al., "Microgrid: A review," 2013 IEEE Global Humanitarian Technology Conference: South Asia Satellite (GHTC-SAS), Trivandrum, 2013, pp. 27-35.
- [10] Zhang and M. Huang, "Microgrid: A strategy to develop distributed renewable energy resource," in Proc. Int. Conf. Electrical and Control Engineering, Sep. 2011, pp. 3520-3523.
- [11] B. Subudhi and R. Pradhan, "A comparative study on maximum power point tracking techniques for photovoltaic power systems," IEEE Trans. Sustain. Energy, vol. 4, no. 1, pp. 8998, Jan. 2013.
- [12] <https://www.mathworks.com>
- [13] IEEE Recommended Practices and Requirements for Harmonic Control in Electrical Power Systems, IEEE Std 519-1992, 1993.

## APPENDIX

1. **PV System:** PV type: Number of Strings in parallel – 66, Numbers of series connected modules in a string – 5, Maximum Power – 305 W , Cells Per Module – 96 Ncell , Voc=64.2 V, Isc=5.96A, At Maximum Power Point, V=54.7 V and I=5.58 A, Temperature Coefficient = -0.27269 %/ deg.C
2. **Battery System:** Type – Lead Acid, Nominal Voltage – 24V, Rated Capacity – 167Ah, Initial state-of-charge – 30%, Battery response time – 20sec, Maximum capacity – 104.1667Ah, Cut-off voltage – 165V, Fully charge voltage – 500V, Nominal discharge current – 20A, Internal resistance – 0.022  $\Omega$ , Capacity at nominal voltage – 31.0278Ah
3. **LC Filter:** R=0.00754  $\Omega$ , L=0.00025 H, and Capacitive kVAR= 10 kVAR
4. **Grid Parameter:** 120 kV, 2500 MVA

## AUTHOR PROFILES

**P. D. Singh** received his Master's degree in Power System Engineering with Gold Medal from North Eastern Regional Institute of Science and Technology, Nirjuli, India, in 2009. Currently, he is an Assistant Professor at Department of Electrical Engineering, North Eastern Regional Institute of Science and Technology, Nirjuli, India.

**Ajay Upadhaya, Michael Simte and Abhishek Sanyal** received their degrees from North Eastern Regional Institute of Science and Technology, Nirjuli, India, in 2019.